Carbohydrate Research 343 (2008) 2433–2438

Contents lists available at ScienceDirect

Carbohydrate Research

journal homepage: www.elsevier.com/locate/carres

A structural and thermal investigation of the inclusion of parabens in heptakis(2,6-di-*O*-methyl)cyclomaltoheptaose ☆

Elise J. C. de Vries, Mino R. Caira *

Department of Chemistry, University of Cape Town, Rondebosch 7701, South Africa

ARTICLE INFO

Article history:
Received 25 March 2008
Received in revised form 10 June 2008
Accepted 12 June 2008
Available online 19 June 2008

Keywords:
Inclusion complex
Heptakis(2,6-di-*O*-methyl)cyclomaltoheptaose
Parabens
Crystal structure

ABSTRACT

The structures of the inclusion complexes formed by heptakis(2,6-di-*O*-methyl)cyclomaltoheptaose and methyl-, ethyl-, propyl- and butyl parabens have been solved and analysed by X-ray diffraction. Each inclusion complex crystallises in the space group $P2_12_12_1$ with $Z = 4$ and a host-to-guest ratio of 1:1. However the packing arrangements and modes of guest inclusion are not equivalent for the four structures. The analytical data indicated that two isostructural pairs, the methyl- and ethyl-paraben complexes, have similar cell parameters that differ from those of the propyl- and butyl paraben complexes. The results of thermogravimetric analysis and differential scanning calorimetry of the complexes are also reported.

1. Introduction

As parabens (4-hydroxybenzoic acid methyl-, ethyl-, propyl- and butyl esters, Fig. 1) have a long history of safety, these are used extensively as inexpensive preservatives in pharmaceutical formulations. Other properties that make parabens so attractive are their broad spectrum of antimicrobial activity: they are active over a wide pH range and are most effective against yeasts and moulds.[1] However, there is a drawback. As the alkyl moiety is lengthened so their antimicrobial potencies increase, their solubility in water decreases. This has led to the use of their sodium salts in formulations, but an alternative approach is cyclodextrin complexation. We have therefore investigated complexation of parabens with cyclomaltoheptaose (β-cyclodextrin, β-CD)[2] and heptakis(2,6-di-*O*-methyl)cyclomaltoheptaose [heptakis(2,6-di-*O*-methyl)-β-cyclodextrin, DIMEB]. This report focuses on the results obtained with the latter host molecule. Unit cell data for these complexes were reported earlier.[3]

DIMEB is produced on methylation of the 2 and 6 hydroxyl groups of β-CD and is attractive for the formation of inclusion complexes owing to its good solubility in both water and organic solvents.[4] However, only a few crystal structures have been reported thus far. The Cambridge Structural Database[5] houses sixteen DIMEB structures, which include an anhydrous form, three hydrated forms and twelve inclusion complexes. DIMEB and its

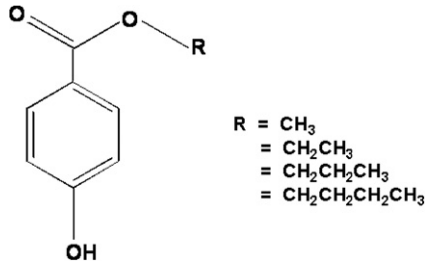

Figure 1. Chemical structures of the paraben molecules.

complexes crystallise in both the monoclinic space group $P2_1$ and the orthorhombic space group $P2_12_12_1$, and various packing modes are observed. As there is less difference in the hydrophilic character of the intra- and intermolecular spaces of DIMEB than β-CD, due to the presence of the methyl groups, the guest molecule(s) can be located either in the cyclodextrin cavity, as with 2-naphthoic acid[6,7] and adamantanol[8] or in the interstitial sites with the cavity occupied by water molecules, as with *p*-iodophenol and *p*-nitrophenol.[9,10] In some instances, such as the carmofur complex, the guest being disordered over two sites is found to be both included in the cavity and located in the intermolecular space.[11] One aspect of the present study was therefore to determine the precise mode of inclusion of the alkyl parabens in the host DIMEB.

This report describes the solid-state inclusion of parabens in DIMEB. The difference between the parabens used in this study lies in the length of the alkyl group. Hence, the aim of this study was to

☆ Also termed heptakis(2,6-di-*O*-methyl)-β-cyclodextrin.

* Corresponding author. Fax: +27 21 689 7499.
E-mail address: Mino.Caira@uct.ac.za (M. R. Caira).

0008-6215/$ - see front matter © 2008 Elsevier Ltd. All rights reserved.
doi:10.1016/j.carres.2008.06.014

investigate the effect of the size, shape and degree of hydrophobicity of the alkyl group on the extent of interaction with DIMEB.

2. Experimental

2.1. Crystallisation

Crystalline complexes were prepared by dissolving an equimolar amount of DIMEB (obtained from Cyclolab, Hungary) with each paraben (purchased from Sigma Chemical Company, USA) in distilled water at room temperature. The resulting unfiltered dilute solutions of the methyl- and ethyl paraben complexes were placed in the oven at 60 °C, whilst the propyl- and butyl paraben solutions were filtered and incubated at approximately 50 °C. Crystals of the methyl- (**1**), ethyl- (**2**), propyl- (**3**) and butyl paraben (**4**) complexes were obtained within two days.

2.2. Thermal analysis

Thermogravimetric and differential scanning calorimetric experiments were performed using a Perkin–Elmer PC-7 Series TGA7 Thermogravimetric Analyser and a DSC7 Differential Scanning Calorimeter, respectively. Samples in the range of 2–4 mg were removed from their mother liquor, blotted dry, accurately weighed, and then heated in open platinum pans for TGA measurements and in sealed, crimped and vented aluminium pans for DSC measurements. A constant heating rate of 10 K min^{-1} and a dry nitrogen purge at 30 cm^3 min^{-1} were employed for both techniques over the temperature range 30–400 °C.

2.3. X-ray data collection

Intensity data were collected on a Nonius Kappa CCD diffractometer from crystals coated with Paratone N oil (Exxon Chemical Co., TX, USA). Data collection (COLLECT software)[12] involved a combination of ϕ- and ω-scans of 0.5° for complexes **1** and **2** and 1.0° for complexes **3** and **4** each with a crystal to detector distance in the range of 58–99 mm. The program DENZO-SMN[13] was used for unit cell refinement and data reduction. Crystallographic data for the four complexes are presented in Table 1. Each complex crystallises in the orthorhombic space group $P2_12_12_1$ with a single DIMEB molecule, its associated guest and water molecules comprising the asymmetric unit.

2.4. Structure solution and refinement

Structure **1** was solved using a Patterson search procedure as implemented in program PATSEE.[14,15] This program uses Patterson and direct methods to orientate and position a fragment of known geometry in a unit cell. The search fragment consisted of the skeleton atoms of a DIMEB molecule from a previously solved complex.[16] After 5000 random positions were refined for 10^6 random orientations, a starting model with favourable statistics was produced from the PATSEE run. Subsequent refinement enabled location of all remaining host atoms: those of the guest molecule and water molecules.

Owing to the isostructurality of complexes **1** and **2**, the structure of **2** was successfully solved using the skeleton atomic coordinates of the DIMEB molecule from structure **1** as trial model. Similarly **3** and **4** were solved using the skeleton atomic coordinates of the DIMEB molecule of the isostructural DIMEB-2-naphthoic acid trihydrate complex.[6,7] All structures were refined by full-matrix least-squares using SHELXL-97.[17]

For each structure, successive difference electron density maps revealed the positions of the remaining non-hydrogen atoms of the host. In some cases atoms were found to be disordered over two positions, and these were modelled using a fixed U_{iso} value and assigning site-occupancy factors of x and $1-x$, with x variable. Distance constraints were placed on the bonds linking these disordered atoms. Almost all the non-hydrogen atoms of the host were refined anisotropically, except for those atoms that were disordered. In each case, the guest phenyl ring was found within the cyclodextrin cavity and refined as a rigid hexagon. The ester substituents of complexes **1** and **2** were disordered over two positions and modelled accordingly. For all four structures, the hydrogen atoms of the host and those attached to the carbon atoms of the guest were geometrically constrained to their parent atoms and refined with linked temperature factors. Hydrogen atoms were

Table 1
Crystal data and structure refinement for the complexes **1**–**4**

	1	**2**	**3**	**4**
Chemical formula	$C_{56}H_{98}O_{35}\cdot C_8H_8O_3\cdot 3.7H_2O$	$C_{56}H_{98}O_{35}\cdot C_9H_{10}O_3\cdot 4.0H_2O$	$C_{56}H_{98}O_{35}\cdot C_{10}H_{12}O_3\cdot 3.9H_2O$	$C_{56}H_{98}O_{35}\cdot C_{11}H_{14}O_3\cdot 3.7H_2O$
Formula weight	1550.2	1569.6	1581.8	1592.2
Crystal system	Orthorhombic	Orthorhombic	Orthorhombic	Orthorhombic
Unit cell constants				
Space group	$P2_12_12_1$	$P2_12_12_1$	$P2_12_12_1$	$P2_12_12_1$
a (Å)	10.6014(1)	10.6560(1)	15.1399(2)	15.3735(2)
b (Å)	15.4760(2)	15.3073(2)	18.8943(3)	18.8114(2)
c (Å)	48.2438(6)	49.0417(6)	28.4009(5)	28.3989(4)
$\alpha=\beta=\gamma$ (°)	90	90	90	90
Volume (Å^3)/Z	7915.2(2)/4	7999.5(2)/4	8124.3(2)/4	8213.0(2)/4
Density$_{(calc)}$ (g cm^{-3})	1.301	1.303	1.293	1.288
Temperature (K)	173(2)	173(2)	173(2)	173(2)
Wavelength (Å)	0.71069	0.71069	0.71069	0.71069
Dimensions (mm)	0.27 × 0.38 × 0.35	0.33 × 0.23 × 0.20	0.45 × 0.39 × 0.17	0.60 × 0.50 × 0.40
θ-range collection (°)	2–25	1–22	2–22	2–21
Index range	$-8\leqslant h\leqslant 12$, $-18\leqslant k\leqslant 10$, $-56\leqslant l\leqslant 55$	$-11\leqslant h\leqslant 11$, $-12\leqslant k\leqslant 15$, $-48\leqslant l\leqslant 29$	$-15\leqslant h\leqslant 15$, $-19\leqslant k\leqslant 19$, $-29\leqslant l\leqslant 29$	$-13\leqslant h\leqslant 15$, $-18\leqslant k\leqslant 12$, $-28\leqslant l\leqslant 25$
Reflections collected	14,594	12,680	19,849	19,801
Independent reflections	9801	7013	9393	8750
Number of parameters	826	604	819	845
R_{int}	0.0196	0.0186	0.0534	0.0295
Goodness of fit	1.037	1.026	1.292	1.028
R_1 [$I>2\sigma(I)$]	0.0904	0.0857	0.1121	0.1007
wR_2	0.2407	0.2122	0.3077	0.2668
Largest diffraction peak and hole (e Å^{-3})	0.76/−0.52	0.73/−0.43	0.50/−0.51	0.57/−0.95

calculated for the C atoms of the host using a riding model with U_{eq}(H) equal to 1.2 U_{eq} or 1.5 U_{eq} of the parent primary and secondary, or tertiary C atoms, respectively. The hydroxyl hydrogen atom of the guests was placed using the rotating group refinement strategy. Due to abnormally long bond distances and abnormally large bond angles found in some of the guest molecules, distance constraints were placed between selected bonded and non-bonded atoms to maintain appropriate values. These values were taken from Lin's paper.[18] In the refinement of the crystal structures, the number of water molecules included in the model was in each case consistent with the estimate of water content based on thermogravimetric analysis (see Section 3.1).

3. Results

3.1. Thermal analysis of the inclusion complexes

The four DIMEB complexes exhibit similar thermogravimetric events. Figure 2 shows the results for complex **1** as representative. Thermogravimetric analysis (TGA) indicated mass losses of 4.3%, 4.6%, 4.4% and 4.2% from ambient temperature up to 100 °C representing water losses of 3.7, 4.0, 3.9 and 3.7 molecules per CD molecule for complexes **1**–**4**, respectively. From 100 to 150 °C, no significant mass loss was observed. Thereafter, there was a mass loss step from 150 °C to 250 °C. This is interpreted as the dissociation of the guest molecule from the host, as the percentage mass loss corresponds to the molecular weight of the paraben in each case. Finally, the remaining sample decomposed at temperatures beyond 300 °C.

Differential scanning calorimetry (DSC) results show a broad endothermic event, A, representing water loss in the range of 30–100 °C, which corresponds to an observed mass loss in the TGA traces. The asymmetric shapes of the dehydration endotherms suggest that water loss from these complexes is a multi-stage process. The anhydrous complex undergoes a smaller endothermic event, B, in the range of 150–230 °C, whose corresponding TGA mass loss is, in each case, consistent with a 1:1 host–guest stoichiometry. The final event, endotherm C, represents fusion of the host followed by decomposition and appears similar in each case.

3.2. Molecular geometries of the host molecules

The geometrical data for the DIMEB molecule of complexes **1–4** are listed in Table 2 (e.s.d.s are in the range of 0.007–0.015 Å for distances and 0.1–0.9° for angles). The seven glucosidic residues have been assigned the G*n* notation with the glucose units numbered 1–7. The average DIMEB conformational parameters of the four inclusion complexes appear to be similar. The DIMEB molecules adopt a rather round and symmetrical structure as deviations of the O(4) atoms from the plane of the macrocycle are small. The average bond distances and angles are in the usual range for the glucopyranose residues. The D-glucose units adopt the $^4C_1$ chair conformation with the O(6) side turned towards the inside of the macrocycle.

In complexes **1** and **2**, the C(6)–O(6) bonds show two types of orientations, the (−)-*gauche* conformation to the C(4)–C(5) and O(5)–C(5) bonds in the G1, G3, G4, G6 and G7 residues and the (+)-*gauche* conformation in the G2 residue. The C(6)–O(6) bond in the G5 residue is disordered, with the major position adopting the (+)-*gauche* conformation, whilst the minor position adopts the (−)-*gauche* conformation. All the O(6)–C(8) bonds are *trans* to the respective C(5)–C(6) bonds, except in the G2 residue and the major position of the G5 residue, where the bond lies *gauche*. All the O(2)–C(7) bonds are directed away from the cavity.

In complexes **3** and **4**, the C(6)–O(6) bonds of the G1, G5, G6 and G7 residues are in the (−)-*gauche* conformation to the C(4)–C(5) and O(5)–C(5) bonds. In complex **3**, the C(6)–O(6) bonds of the G2 and G4 residues are in the (+)-*gauche* conformation. The C(6)–O(6) bond of the G3 residue is in a *trans* conformation. In complex **4**, the C(6)–O(6) bond of the G2 residue is in the (+)-*gauche* conformation. The O(6) atoms of the G3 and G4 residues are disordered over two sites. Both the major and minor positions of the atoms of the G4 residue are in the (+)-*gauche* conformation. The major position of the G3 residue assumes the (+)-*gauche* conformation, whilst the minor position assumes the (−)-*gauche* conformation. All the O(6)–C(8) bonds, including the disordered CH_3 on O(6) of

Table 2
Geometrical parameters for the DIMEB molecules

Residue	D[a] (Å)	ϕ[b] (°)	d[c] (°)	α[d] (Å)	D_3[e] (Å)	τ[f] (°)
Complex **1**						
G1	4.28	127	3.2	0.02	2.76	0.6
G2	4.41	124	−4.1	−0.10	2.86	12.5
G3	4.48	134	−1.4	0.04	2.82	11.2
G4	4.38	128	3.9	0.10	2.82	7.8
G5	4.31	125	0.9	−0.07	2.92	9.7
G6	4.44	129	−6.3	−0.08	2.93	14.5
G7	4.41	133	3.4	0.11	2.84	5.4
Complex **2**						
G1	4.29	127	4.5	0.04	2.72	0.5
G2	4.36	123	−5.1	−0.13	2.86	13.8
G3	4.51	134	−1.9	0.04	2.79	11.5
G4	4.39	129	5.2	0.12	2.81	9.3
G5	4.27	124	0.2	−0.09	2.93	8.7
G6	4.45	128	−6.2	0.09	2.87	14.1
G7	4.44	134	2.8	0.12	2.85	5.0
Complex **3**						
G1	4.43	131	6.7	−0.03	2.88	7.1
G2	4.25	125	−11.0	−0.23	2.80	14.5
G3	4.55	132	2.1	0.13	2.89	14.7
G4	4.30	127	6.7	0.14	2.87	4.8
G5	4.43	128	−2.3	−0.12	2.97	15.6
G6	4.38	130	−6.5	−0.04	2.88	16.0
G7	4.36	127	4.3	0.17	2.82	7.0
Complex **4**						
G1	4.41	130	6.2	−0.02	2.91	7.9
G2	4.34	125	−10.6	−0.21	2.80	15.1
G3	4.41	133	3.4	0.12	2.87	16.4
G4	4.33	126	4.4	0.09	2.87	5.3
G5	4.44	128	−1.0	−0.10	2.95	14.9
G6	4.35	130	−6.1	−0.05	2.86	16.1
G7	4.38	127	3.7	0.15	2.78	6.3

[a] Glycosidic O4n···O4(n + 1) distance.
[b] O4(n − 1)···O4n···O4(n + 1) angle.
[c] O4(n − 1)··O4n···O4(n + 1)···O4(n + 2) torsion angle.
[d] Deviation of atoms O4n from the least-squares planes (mean e.s.d. 0.007 Å).
[e] Inter-ring hydrogen bond O(2n)···O(3n − 1) distances (mean e.s.d. 0.010 Å).
[f] Tilt angle between the mean O(4) plane and the mean plane through the six pyranose ring atoms, namely C(1), C(2), C(3), C(4), C(5) and O(5) of each glucose unit (mean e.s.d. 0.2°).

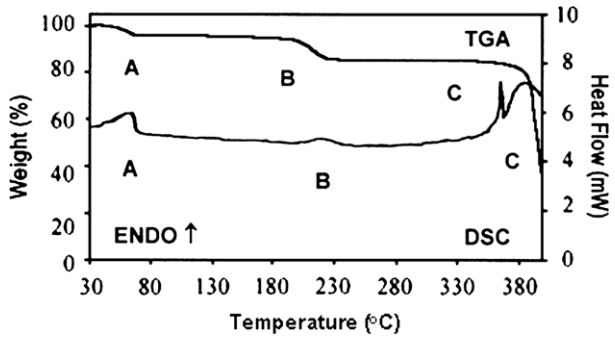

Figure 2. TGA and DSC traces for complex **1** as representative.

the G5 residue, are *trans* with respect to the C(5)–C(6) bonds, except the O(6)–C(8) bond of the G3 residue of complex **3**, which is *cis*. All the O(2)–C(7) bonds are directed away from the cavity.

All the glucose units are orientated *syn*, and thus the O(2) and O(3) atoms of adjacent glucose units form seven intramolecular O(2)···O(3′) hydrogen bonds that contribute to the conformational stability of the cyclodextrin macrocycle. Additionally, a series of intramolecular C–H···O hydrogen bonds maintains the conformation of the DIMEB molecule. The cohesion of the structure is ensured by intermolecular C···O contacts involving the O(2), O(3) and O(6) groups of the macrocycle.

3.3. Molecular geometries of the host molecules

The mode of guest inclusion is analogous for the isostructural complexes **1** and **2**. Figure 3 shows the structure of **1** as representative. The guest is almost completely enclosed in the cyclodextrin cavity, with its long axis orientated in the direction of the molecular axis of the host. The phenolic hydroxyl group of the guest molecule is located at the secondary rim. The ester moiety is located at the narrower primary rim and in both structures is found to be disordered over two positions. The phenyl ring of the guest is almost perpendicular to the mean O(4) plane with angles of 88.9(2)° and 87.3(2)° for complexes **1** and **2**, respectively.

3.4. Guest conformation and mode of inclusion

Similarly, the modes of guest inclusion for complexes **3** and **4** are analogous, but different from the arrangements in **1** and **2**. Figure 3 shows the structure of **3** as representative of this isostructural pair. The phenolic hydroxyl group of the guest and the aromatic ring now extend well beyond the primary rim of the host. The phenyl rings of the guests form angles of 55.9(2)° and 53.0(2)° with the mean O(4) plane for complexes **3** and **4**, respectively. This allows the hydrophobic alkyl chain to be located at the hydrophobic inner surface of the cyclodextrin cavity. This orientation corresponds to the model of Lichtenthaler et al.[19,20] in that the hydrophilic and hydrophobic portions of the guest align with the hydrophilic and hydrophobic portions of the host, respectively. This represents a significantly different mode of inclusion from that observed in the previous two complexes. Differences are also observed in hydrogen-bond formation. In complexes **1** and **2**, the hydroxyl oxygen atom of the guest forms three hydrogen bonds to the host molecules in symmetry-related positions, and it is also hydrogen bonded to one water molecule. Instead, in complexes **3** and **4** the hydroxyl oxygen atom of the guest is hydrogen bonded to one water oxygen atom and to two atoms on the host molecule.

3.5. Water interactions

The percentage water in each structure was measured using thermogravimetric analysis. All the water molecules are situated at the periphery of the cyclodextrin molecule, filling the intermolecular space between complex units. One water molecule is within hydrogen-bonding distance of the guest hydroxyl oxygen atom in each structure. The remaining waters are either within hydrogen-bonding distance of a host oxygen atom or another water molecule.

3.6. Molecular packing

Complexes **1** and **2** stack in columns in a head-to-tail mode, forming what appear to be continuous channels along the *a*-axis in a modified herringbone scheme. This is shown in Figure 4 (top). The herringbone chains form sheets parallel to the *bc*-plane which are stacked along the *a*-axis. However, the twofold screw axis parallel to the *a*-axis does not pass through the host cavity, and, therefore, complex units related by the 2_1-axis in this direction are members of adjacent columns. The consequence of this is a much shorter cell length *a* than the cell lengths *b* in complexes **3** and **4**, and, therefore, successive complex units within a column are related by a unit cell translation rather than by a twofold screw axis.

The molecules of complexes **3** and **4** are stacked along the *a*-axis in a zigzag type pattern, and the twofold screw axis parallel to this direction passes through the host cavity (Fig. 4, bottom). The O(6)

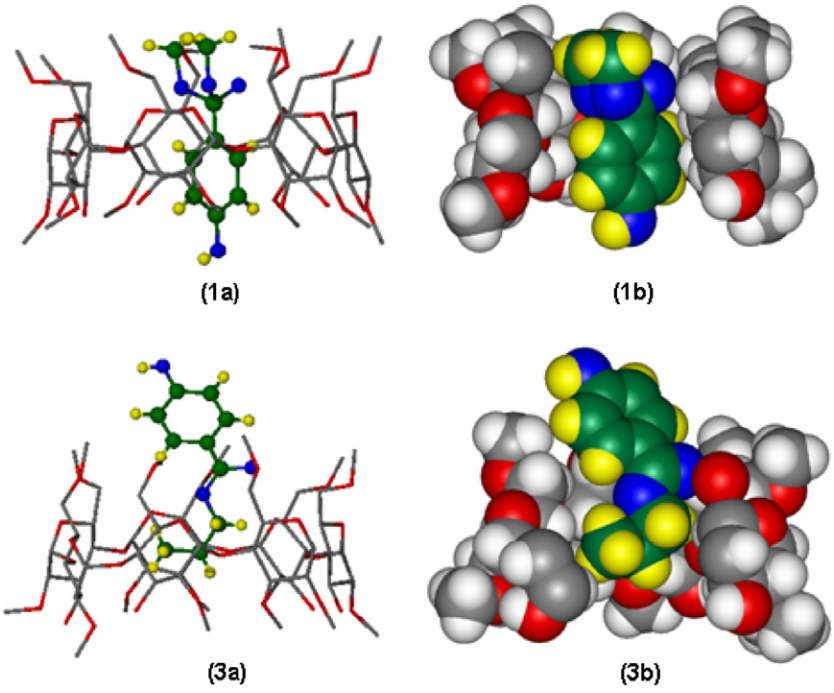

Figure 3. Representative structures **1** and **3** shown in (a) ball-and-stick mode, and (b) sectioned view in space-filling mode.

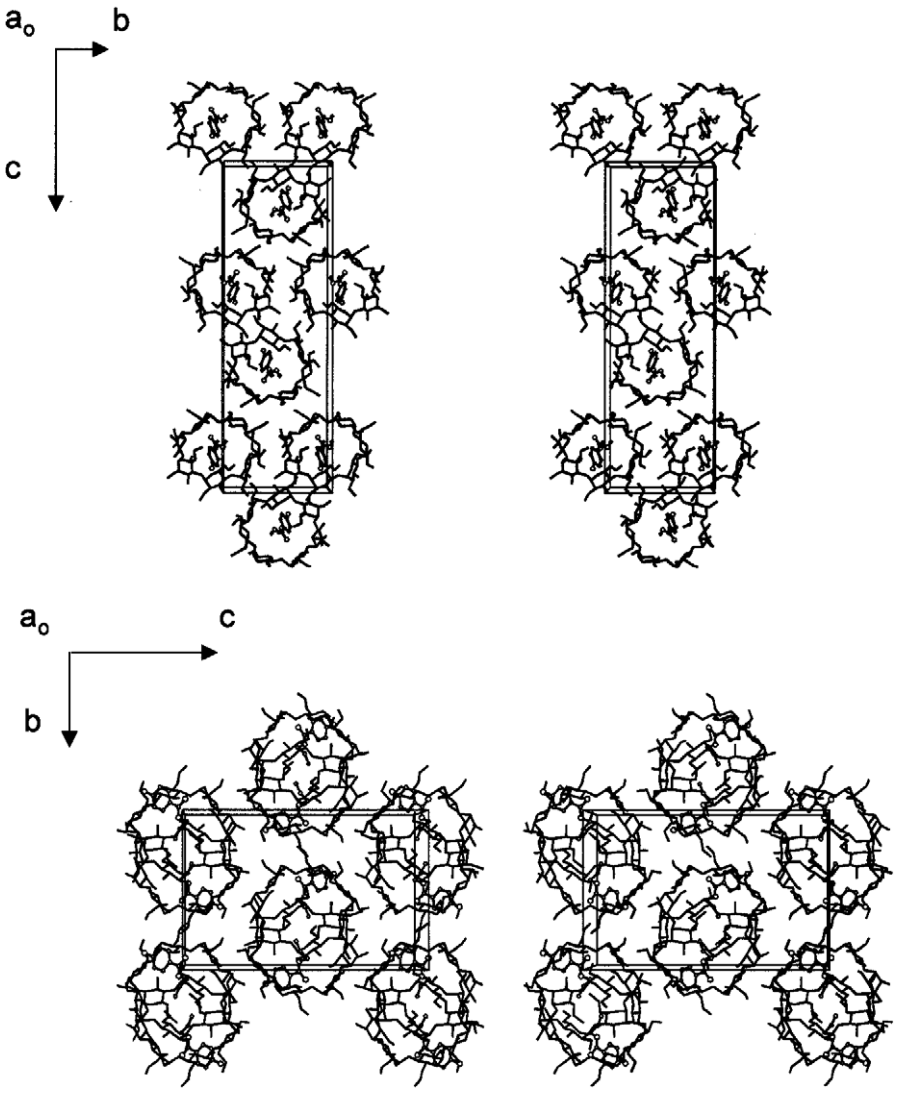

Figure 4. Stereo packing diagram of complex **1** (top) and **3** (bottom), *a*-axis projection.

side of the cavity is open to the intermolecular space, where the guest is located. In complex **3**, the O(6) side is partially blocked as the primary methoxy moiety of the G3 residue is in the *cis* conformation, whilst on the G4 residue it protrudes into the cavity 'above' it. In **4**, the primary O(6)–CH_3 group on both the G3 and G4 residues protrudes into the CD cavity 'above' it. Thus, the cavity is partially filled by the guest and the O(6)–CH_3 group of an adjacent molecule related by the twofold screw axis parallel to *a*.

4. Discussion

The combination of thermal analysis and X-ray analysis has shed light on both the thermal stability and the intimate details of the structures of complexes **1–4**. Combined DSC and TGA analyses indicated a common degradation pathway on heating the crystals, namely dehydration, subsequent release of the included guest molecules and final fusion and decomposition of the host compound. Crystal water content determined by TGA served as primary data for ensuring accurate modelling of the water molecules in the crystal structures.

The crystal data show that the four structures can be divided into two isostructural pairs *viz*., **1** and **2** as one pair and **3** and **4** as the other. The term 'isostructural' is used as one pair exhibits a similar internal arrangement of molecules, has a comparable hydrogen bonding network and has an analogous crystal packing motif.[21,22] This is evident from the data and is further confirmed by comparing the X-ray powder diffraction patterns computed from the refined single-crystal X-ray structures.

Distinctly different modes of inclusion of the guests in the two isostructural series were established from single-crystal X-ray diffraction experiments. From this study, it is evident that the size, shape and degree of hydrophobicity of the alkyl chain affect the packing arrangement and extent of interaction of the guest with the host molecule. Steric interactions influence the orientation of the guest in complexes **1** and **2**, whilst hydrophobicity plays an important role in the orientation of the propyl and butyl paraben guests in complexes **3** and **4**.[19,20]

Whilst each member of the series of paraben guests also forms a 1:1 inclusion complex with the native host β-CD,[2] the resulting complexes have fundamentally different structures from those of complexes **1–4** reported here. All of the former complexes are dimeric, two guest molecules being encapsulated within the large cavity generated by two β-CD molecules that are hydrogen bonded (O–H···O) to one another through their secondary faces. In addition, the extent of guest disorder in the series of β-CD complexes is greater than that observed in the DIMEB complex series reported

here. In the case of methyl paraben as guest, two distinct β-CD 1:1 inclusion complexes that crystallise in different space groups were thermally and structurally characterised and shown to have significantly different thermal stabilities.[23] This finding underscored the practical importance of controlling crystallisation conditions during the preparation of CD inclusion complexes.

5. Supplementary data

The CIF files for the complexes have been deposited with the Cambridge Crystallographic Data Centre (CCDC 682352–682355 for complexes **1**–**4**, respectively). These data may be obtained, on request, from the CCDC, 12 Union Road, Cambridge CB2 1EZ, UK. Tel.: +44-1233-336408; fax: +44-1233-336033; e-mail: deposit@ccdc.cam.ac.uk.

Acknowledgements

M.R.C. and E.D.V. thank the NRF (Pretoria) and the University of Cape Town for financial assistance.

References

1. Wade, A., Weller, P. J. Handbook of Pharmaceutical Excipients, 2nd ed.; 1994; American Pharmaceutical Association: Washington, DC; p 49.
2. de Vries, E. J. C.; Caira, M. R.; Bogdan, M.; Farcas, S. I.; Bogdan, D. *Supramol. Chem.*, in press.
3. Caira, M. R.; de Vries, E. J. C.; Bogdan, M.; Bogdan, D.; Farcas, S. I. *Studia Universitatis Babes-Bolyai* **2003**, *48*, 95–102. Physica, special issue 1, XL VIII.
4. Harata, K. In *Inclusion Compounds*; Atwood, J. L., Davies, J. E. D., MacNicol, D. D., Eds.; Oxford University Press: Oxford, 1991; Vol. 5; pp 312–344.
5. *Cambridge Structural Database and Cambridge Structural Database System, Version 5.29*; Cambridge Crystallographic Data Centre, University Chemical Laboratory; Cambridge, England, November 2007.
6. Harata, K. *J. Chem. Soc., Chem. Commun.* **1993**, 546–547.
7. Harata, K. *Chem. Commun. (Cambridge)* **1999**, 191–192.
8. Czugler, M.; Eckle, E.; Stezowski, J. J. *J. Chem. Soc., Chem. Commun.* **1981**, 1291–1292.
9. Harata, K. *Bull. Chem. Soc. Jpn.* **1988**, *61*, 1939–1944.
10. Harata, K. *Chem. Lett.* **1984**, 1641–1644.
11. Harata, K.; Hirayama, F.; Uekama, K.; Tsoucaris, G. *Chem. Lett.* **1988**, 1585–1588.
12. Hooft, R. COLLECT; Nonius BV: Delft, The Netherlands, 1998.
13. Otwinowski, Z.; Minor, W. *Methods Enzymol.* **1997**, *276*, 307–326.
14. Egert, E. *Acta Crystallogr., Sect. A* **1983**, *39*, 936–940.
15. Egert, E.; Sheldrick, G. M. *Acta Crystallogr., Sect. A* **1985**, *41*, 262–268.
16. Caira, M. R.; Bourne, S. A.; Mvula, E. N. *Biologicheskii Zhurnal Armenii* **2001**, *53*, 148–158.
17. Sheldrick, G. M. SHELXL-97; University of Göttingen: Germany, 1997.
18. Lin, X. *J. Struct. Chem.* **1983**, *2*, 213.
19. Lichtenthaler, F. W.; Immel, S. *Starch* **1996**, *48*, 145–154.
20. Lichtenthaler, F. W.; Immel, S. *Starch* **1996**, *48*, 225–232.
21. Fábián, L.; Kálmán, A. *Acta Crystallogr., Sect. B* **1999**, *55*, 1099–1108.
22. Kálmán, A.; Párkányi, L. In *Advances in Molecular Structure Research*; Hargittai, M., Hargittai, I., Eds.; JAI Press: Stamford, Connecticut, 1997; Vol. 3; pp 189–226.
23. Caira, M. R.; de Vries, E. J. C.; Nassimbeni, L. R. *Chem. Commun. (Cambridge)* **2003**, 2058–2059.